

Surface Nitriding of Light Metals using Electron-Beam-Excited-Plasma (EBEP) Source

Ryuta ICHIKI, Yuusuke KUBOTA, Masashi YOSHIDA, Yuji FUKUDA, Yasuyuki MIZUKAMO, and Tamio HARA

Toyota Technological Institute, Nagoya 468-8511, Japan

(Received: 27 August 2008 / Accepted: 27 January 2009)

The electron-beam-excited-plasma (EBEP) source exhibits a number of advantageous properties in surface nitriding of light metals such as titanium, ensuring that the technology of EBEP source is a highly promising candidate for novel practical application of surface nitriding for light metals. We have found that the EBEP source can perform low-temperature surface nitriding of titanium without deteriorating the strength of the bulk substrate. Moreover, the compound layer formed on the outmost surface is composed of only Ti₂N, which will provide a greater fracture strength than TiN.

Keywords: electron-beam-excited-plasma, EBEP, nitriding, surface hardening, titanium, light metal

1. Introduction

The electron-beam-excited-plasma (EBEP) source is a unique electron beam source that can produce amperes of dc electron beam with low kinetic energy around 100 eV [1]. Since electrons with this range of energy possess large impact dissociation or ionization cross-sections of gas molecules, the EBEP source has been widely utilized for selectively hastening specific chemical reactions in the gas phase. The extremely versatile characteristics have been spreading its application into wide variety of fields including Ar⁺ laser [2], ion sources [1], etching [3], chemical vapor deposition (CVD) [4], physical vapor deposition (PVD) [5], and surface treatment/cleaning [6]. Lately, EBEP sources have been actively researched for nitriding of steel [7-11], one of the surface-hardening heat treatments. In steel nitriding, nitrogen atoms are introduced into the surface of sample to form the compound layer (such as Fe₄N) and the diffusion layer (a solid solution composed of metal and nitrogen atoms), leading to high surface hardness, great wear resistance, long fatigue life, etc [12]. The key factor in nitriding is to produce a great number of N atoms [13]. In general, a high dissociation efficiency of N₂ molecules was hard to gain by means of thermal-electron bombardment because of its high bonding energy of 9.8 eV and the channeling of input energy into the vibrational manifold of N₂(X¹Σ_g⁺, ν) [14]. Therefore, the utilization of the EBEP source is most appropriate. In fact, a number of studies have revealed that the nitrogen EBEP exhibits high performance in nitriding of steels [7-11]. This fact has triggered the application of the EBEP nitriding also to nonferrous, light metals.

Light metals, especially titanium (Ti), aluminum (Al), and their alloys find wide industrial applications because of extremely attractive properties such as high strength to

weight ratio and very good corrosion resistance. However, their low surface hardness and poor wear resistance have been limiting wider potential applications. To overcome these disadvantages, research for improving the surface property is promoted worldwide. In particular, nitriding assisted by plasmas is a promising candidate since a native oxide layer of Ti or Al surface, which plays a role of a barrier against nitriding, can be removed by ion sputtering process before/during nitriding treatment [15]. Nevertheless, contrary to the well-established nitriding technology for steels, that for nonferrous metals is still in the developmental phase.

Nitriding of titanium and its alloys have been studied for several decades by means of gas nitriding and ion nitriding [16-20]. A number of past studies adopted the treatment temperature T_s around/more than 1000 °C for enhancing the growth rate of the nitrided layer [18]. The temperature above the β-transition temperature 885 °C, however, provides grain coarsening, inhomogeneous microstructure, cracking, etc [17]. In view of the proven outstanding performance of the EBEP source in steel nitriding, we are conducting research work on application of the EBEP source to Ti nitriding at a low T_s of 720 °C, much lower than the β-transition. Here, we present the first report on possibility of Ti nitriding by using the EBEP source.

2. Experimental Procedure

Figure 1(a) illustrates the principle of the compact EBEP source. The source is divided into three regions: the discharge region, the electron-acceleration region, and the EBEP region. A dc Ar plasma, which plays a role of the electron source for electron beam extraction, is produced in the discharge region between the hot cathode K of a LaB₆

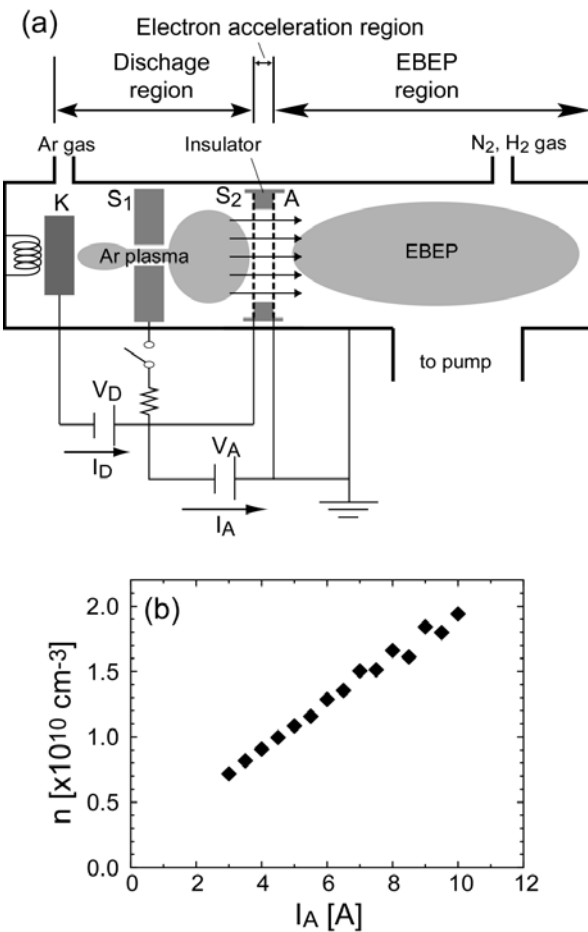


Fig.1 (a) Schematic of the compact EBEP source. K – cathode, S_1 – subanode, S_2 – anode, and A – electron accelerator, V_D – discharge voltage, I_D – discharge current, V_A – electron acceleration voltage, I_A – apparent electron beam current. (b) Produced EBEP density n vs I_A . Probe characteristics were detected in the EBEP region at a distance of 50 cm from the electron accelerator. A cylindrical Langmuir probe of 1 mm in diam and 2 mm in length made of tungsten was used.

disk and the anode S_2 . V_D and I_D are the discharge voltage and current in the Ar plasma production, respectively. (The subanode S_1 is the structure used only in igniting the Ar plasma [21].) Electron beam is extracted from the Ar plasma and accelerated in the electron acceleration region by applying the bias voltage V_A to the electron accelerator A with respect to S_2 . The electron beam energy is controlled by adjusting the difference between V_A and the space potential of the Ar plasma. I_A is the apparent electron beam current, which is the total of the actual electron beam current and the electron flow absorbed by the electron accelerator. The value of I_A can be controlled by varying the Ar plasma density, namely I_D , where the electron extraction efficiency $I_A/I_D \sim 0.5$. Direct bombardment of

the electron beam on N_2 gas produces a nitrogen EBEP containing a great deal of N. Note that through the present work the electron beam energy is set to 80 eV which corresponds to the peak of electron impact N_2 dissociation cross-section. As shown in Fig. 1(b), the EBEP density produced is linearly increased with I_A . Although the present experiment did not involve *in-situ* measurement of the density of N atoms, the N density has been demonstrated to increase in proportion to I_A in other EBEP devices [9,21,22]. Here, I_A is set to 8 A because of the upper limit of the device. A remarkable fact is that a small fraction of positive ions produced in the EBEP region are accelerated toward S_2 to proceed into the electron acceleration region. This ion influx cancels out the space charge limitation in the region, thereby allowing high-current, low-energy electron beam extraction. The electron temperature T_e and the space potential ϕ_p are 2.5 eV and -1 V, respectively, and are independent of I_A . The EBEP region is composed of a quartz cylindrical tube (15.5 cm in internal diameter and 80 cm in length) because silica has a low probability of N atom surface recombination, $\gamma < 10^{-4}$ [23], while for stainless-steel $\gamma < 10^{-2}$ [14]. Besides, the quartz tube is surrounded by an external furnace for nitriding experiments.

Pure Ti (JIS grade 2) is employed as the sample material for observing basic property. Samples are circular plates of 20 mm in diameter and 4 mm in height. The samples were polished to mirror finish, and then degreased ultrasonically in acetone bath. A sample was put on a quartz plate located in the EBEP region at 50 cm from the electron accelerator, and was connected to a sheathed thermocouple to monitor T_s . The value of T_s was adjusted to 720 °C by the external furnace. Before nitriding treatment, the native oxide layer was sputter-removed in an Ar EBEP at $V_s = -200$ V for 1 h. In the nitriding treatment, the flow rates of Ar, N_2 , and H_2 gases were 20, 20, and 15 sccm, respectively, where the pressure of the EBEP region was 0.24 Pa. The superimposition of H_2 gas was made to keep the sample surface clean by reducing oxide due to the residual O_2 gas [20]. V_s was kept to -200 V during the nitriding treatment. The thickness of the compound layer is observed by optical microspectrometry and its phase constitution is determined by X-ray diffraction (XRD) using Co $K\alpha$ radiation. The thickness of the diffusion layer is detected from the depth profile of hardness measured by a micro-Vickers hardness tester with a load of 5 g.

3. Results and Discussion

Figure 2 shows a micrograph of an etched cross-section of a nitrided sample. A discrete thin layer is seen on the outmost surface, that is the compound layer. The compound layer becomes thick as the treatment time t increases, as shown in Fig. 3. After $t = 4$ h, however, the

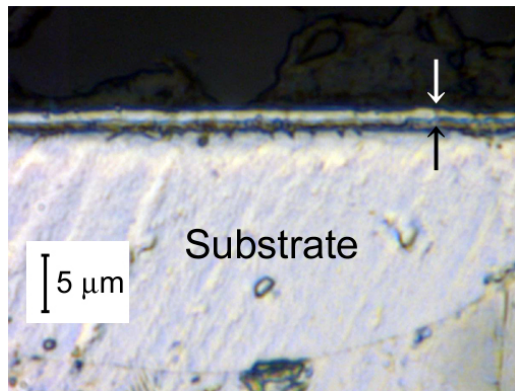


Fig.2 Micrograph of cross-section of Ti sample nitrided for 16 h. An etching process was performed with 100 ml H₂O + 2 ml HF + 5 ml H₂O₂ for 1 min to make the compound layer optically visible.

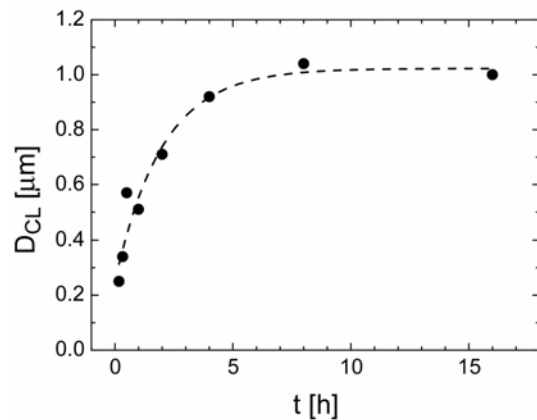


Fig.3 Thickness D_{CL} of the compound layer formed on pure Ti as a function of treatment time t .

thickness is saturated at 1 μm. This tendency cannot be directly expected by the diffusion controlling mechanism, in which the layer thickness is controlled by Fick's law of diffusion to increase in proportion to $t^{1/2}$. It was reported in a study of steel nitriding that consideration of ion sputtering effect removing the compound layer can result in a saturation behavior of the layer growth [24]. Since there is no database of the sputtering rate of Ti₂N by Ar/N₂ as far as the authors know, experimental evaluation of the sputtering rate will be the first task.

Figure 4 shows the time evolution of XRD patterns for the sample surface. It is remarkable that only the peaks corresponding to Ti₂N is growing and no peak of TiN is found. In contrast, other types of Ti nitriding such as gas or plasma nitriding form a TiN layer or TiN-Ti₂N layers [16-20]. Since Ti₂N was reported to outperform TiN in fracture strength owing to a relatively low hardness [20], our result indicates a potential advantage of the EBEP nitriding. Experimental research on fracture and fatigue

strength of Ti nitrided with EBEP is ongoing. In addition, the mechanism of selective formation of Ti₂N in the case has to be investigated in the context of the N density, T_s , and V_s .

Figure 5 shows Vickers microhardness profiles on the cross-sections of nitrided samples. Here the increment of the hardness from the original hardness 200 Hv_{0.005} is shown. A hardened layer is found to grow temporally, demonstrating that the EBEP nitriding has successfully produced the diffusion layer in Ti. The surface layer became almost doubled in hardness. The hardness decreases through the diffusion layer and approaches to the original hardness, as can be seen also in a diffusion layer of steel. The gradually decreasing profile of hardness is a fundamental point to improve fracture and fatigue strength of the nitrided layer. Here, we see that the depth profile of hardness is becoming more gentle as t increases. For

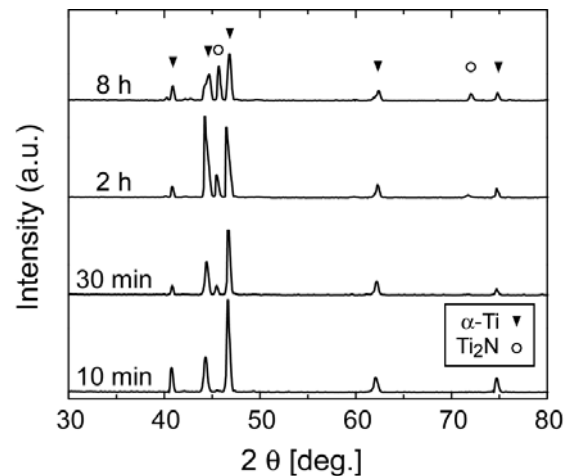


Fig.4 X-ray diffraction patterns of nitrided Ti surface for several treatment times.

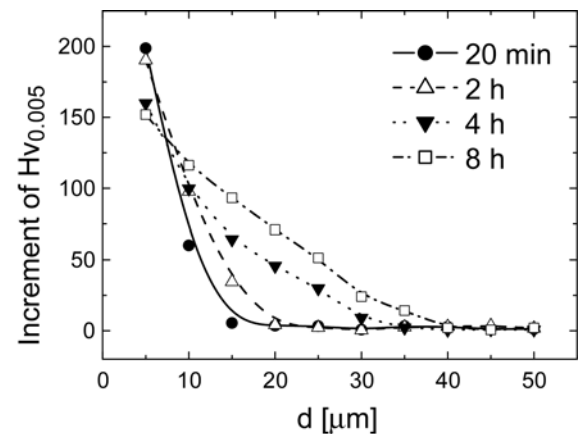


Fig.5 Time evolution of hardness profile of nitrided Ti as a function of the depth from the surface d . The hardness of as-received sample is 200 Hv_{0.005}. Each dot is the averaged value of three-time measurements.

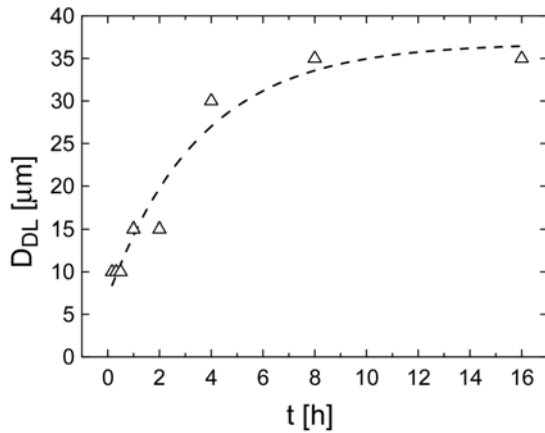


Fig.6 Thickness D_{DL} of the diffusion layer formed on pure Ti as a function of treatment time t . The value of D_{DL} is defined with the distance between the surface and the beginning point of hardening.

optimizing the strength of nitrided workpieces we have to find out the growth mechanism of the diffusion layer to control the hardness profile precisely. However, we have revealed that the growth of the diffusion layer is inconsistent with the diffusion controlling mechanism as well as the compound layer. As shown in Fig. 6, the diffusion layer also exhibits saturation of growth. The growth of the diffusion layer should not connect to the effect of ion sputtering directly. Thus, we have to consider other possible effects such as the barrier effect, in which the already-formed compound layer plays a barrier role against N atom penetration. In any case, the diffusion layer approaches to 35 μm in thickness for t of 8 h. The thickness and the treatment time are both adequate for industrial use. A higher T_s provides a faster growth rate of the diffusion layer, but the detail will be presented elsewhere. We are planning nitriding of Ti alloys such as Ti-6Al-4V to compare the performance of the EBEP source with other nitriding treatment [19].

4. Conclusions

In this article, we have presented the first result of nitriding of titanium using the EBEP source. The EBEP source exhibited a capability of surface nitriding of titanium even at a treatment temperature of 720 °C much lower than the β -transition of Ti. The diffusion layer grew to 35 μm in thickness for the treatment time of 8 h. On the other hand, the compound layer had at most 1 μm in thickness. More importantly, its phase was only Ti₂N without TiN, indicating a possibility to improve fracture strength of the compound layer.

These new findings ensure the EBEP nitriding as a powerful tool for novel surface hardening technology for light metals. To specify the detailed mechanism of nitrided-layer growth, further experiments and analyses

are running. Moreover, we have a project to investigate the feasibility of industrial mass nitriding using the EBEP source.

Acknowledgment

The authors are grateful to Dr. Y. Imada and Prof. M. Sasaki for technical support on chemical composition analyses and optical microspectrometry.

- [1] T. Hara, M. Hamagaki, A. Sanda, Y. Aoyagi, and S. Namba, J. Vacuum Sci. Technol. B **5**, 366 (1987).
- [2] T. Hara, Y. Sadamoto, M. Hamagaki, T. Ohgo, and T. Dote, Jpn. J. Appl. Phys. **22**, L379 (1983).
- [3] K. Takeda, T. Ohta, M. Ito, and M. Hori, J. Vac. Sci. Technol. A **24**, 1725 (2006).
- [4] M. Ban, T. Hasegawa, S. Fujii, and J. Fujioka, Diamond Relat. Mater. **12** 47, (2003).
- [5] S. Ozawa and M. Hamagaki, Vacuum **74**, 417 (2004).
- [6] Y. Hashimoto, Y. Osato, M. Tanaka, M. Hamagaki, and T. Sakakibara, Jpn. J. Appl. Phys. **41**, 2249 (2002).
- [7] K. Taniguchi, M. Hashimoto, T. Hishida, H. Shoyama, and T. Hara, Proc. 27th Int. Conf. Phenomena in Ionised Gases, 2005, No. 10-409 (CD-ROM).
- [8] L. Liu, A. Yamamoto, T. Hishida, T. Hara, and H. Tsubakino, Mater. Trans. **46**, 687 (2005).
- [9] H. Shoyama, T. Hishida, T. Hara, Y. Dake, T. Mori, H. Nagai, M. Hori, and T. Goto, J. Vac. Sci. Technol. A **24**, 1999 (2006).
- [10] Y. Hara, Y. Yoshikawa, T. Hara, and P. Abraha, Jpn. J. Appl. Phys. **46**, L1077 (2007).
- [11] P. Abraha, Y. Yoshikawa, and Y. Katayama, "Surface modification of steel surfaces by electron beam excited plasma processing," Vacuum, in press.
- [12] Y. Sun and T. Bell, Mater. Sci. Eng. A **140**, 419 (1991).
- [13] T. Czerwiec, H. Michel, and E. Bergmann, Surf. Coat. Technol. **108-109**, 182 (1998).
- [14] S. F. Adams and T. A. Miller, Plasma Sources Sci. Technol. **9**, 248 (2000).
- [15] M. Moradshahi, T. Tavakoli, S. Amiri, and Sh. Shayeganmehr, Surf. Coat. Technol. **201**, 567 (2006).
- [16] M. Raaif, F. M. El-Hossary, N. Z. Negm, S. M. Khalil, and P. Schaaf, J. Phys.: Condens. Matter. **19**, 396003 (2007).
- [17] A. Zhecheva, S. Malinov, and W. Sha, Surf. Coat. Technol. **201**, 2467 (2006).
- [18] A. Zhecheva, S. Malinov, and W. Sha, JOM **59**, 38 (2007).
- [19] F. Yildiz, A. F. Yetim, A. Alsaran, A. Çelik, Surf. Coat. Technol. **202**, 2471 (2008).
- [20] T. Nanbu and M. Takemoto, J. Surf. Fin. Soc. Jpn. **46**, 443 (1995) [in Japanese].
- [21] S. Tada, S. Takashima, M. Ito, M. Hamagaki, M. Hori, and T. Goto, Jpn. J. Appl. Phys. **41**, 4691 (2002).
- [22] K. Taniguchi, M. Sugimoto, S. Masuko, T. Kobayashi, M. Hamagaki, P. Abraha, and T. Hara, Jpn. J. Appl. Phys. **39**, L999 (2000).
- [23] Y. C. Kim and M. Boudart, Langmuir **7**, 2999 (1991).
- [24] E. Roliński and G. Sharp, J. Mater. Eng. Perform. **10**, 444 (2001).